https://ntrs.nasa.gov/search.jsp?R=20160011117 2020-05-09T09:34:43+00:00Z

A Toolbox of Metrology-based Techniques for Optical System Alignment

Phillip Coulter[1], Raymond G. Ohl[1], Peter N. Blake[1], Brent J. Bos[1], William L. Eichhorn[2], Jeffrey S. Gum[1], Theodore J. Hadjimichael[1], John G. Hagopian[3], Joseph E. Hayden[4], Samuel E. Hetherington[1], David A. Kubalak[1], Kyle F. Mclean[5], Joseph McMann[6], Kevin W. Redman[6], Henry P. Sampler[1], Greg W. Wenzel[6], Jerrod L. Young[1]

[1]NASA Goddard Space Flight Center
[2]Genesis Engineering Solutions Inc
[3]John Hagopian Engineering, LLC
[4]Sigma Space Corporation
[5]Pinnacle Engineering & Management Solutions, LLC
[6]Sierra Lobo, Inc

ABSTRACT

The NASA Goddard Space Flight Center (GSFC) and its partners have broad experience in the alignment of flight optical instruments and spacecraft structures. Over decades, GSFC developed alignment capabilities and techniques for a variety of optical and aerospace applications. In this paper, we provide an overview of a subset of the capabilities and techniques used on several recent projects in a "toolbox" format. We discuss a range of applications, from small-scale optical alignment of sensors to mirror and bench examples that make use of various large-volume metrology techniques. We also discuss instruments and analytical tools.

Keywords: JWST, metrology, optical alignment, OVIRS, spacecraft alignment

1. INTRODUCTION

GSFC has significant heritage in building and aligning spacecraft and space flight optical instruments. We discuss techniques used at GSFC and various recent applications. Planning the development of a spacecraft or optical system includes the development of an "alignment plan" Guyer (2001)[1], for example, presents an illustrative work flow showing the steps associated with developing an alignment plan for an optical system (Figure 1**)**. Metrology tools, techniques, and data reduction and analysis algorithms would be considered in Guyer's lower left blocks labeled "Alignment plan/procedure" and "Step back," then evaluated again in further iterations of the loop on the left of his flow chart. Often, one choses metrology interfaces, etc., such that more than one type of metrology system can be used, in case there are changes later during the build phase to availability, requirements, or something unforeseen develops (i.e., there is strength in flexibility). Metrology systems, optical test/verification methods, and optical ground support equipment are often considered together in the development loop and synergies sought.

This paper discusses measurement-related tools for consideration when developing an alignment plan and useful for accomplishing a plan or reacting to problems during the implementation. Some measurement instruments, alignment techniques and analysis tools are discussed in the following sections. We do not discuss interferometry or wavefront sensing and similar, optical-only techniques --- those subjects are broad and well treated by others. We focus on techniques and instruments that are less used by optical engineers and usually not covered in classical optical engineering curricula. These are techniques that would be employed to accomplish alignment before high-precision optical testing, like interferometry or image testing, is used to fine-tune and optical system or verify performance.

One of the first steps in building an optical system is the definition of a coordinate system (Section 2). Section 3 focuses on the various measurement instruments available to the engineer and their capabilities. We cover component characterization and how the results are applied to the integration phase in Section 4. Some analysis tools are described

as well as a few recent applications in Section 6. Section 6 offers a brief discussion on several applications of recent flight projects at GSFC.

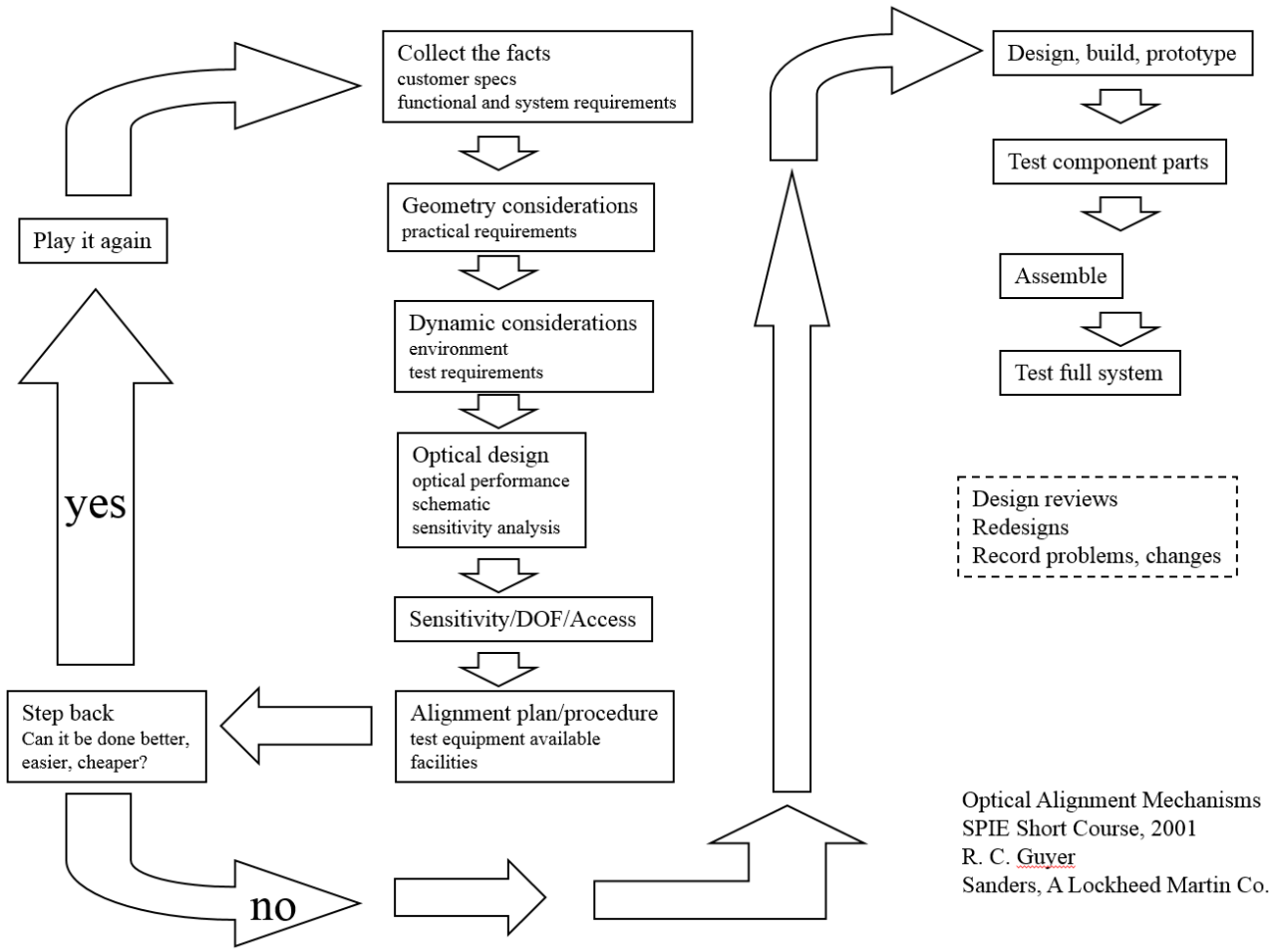

Figure 1. Process flow for developing an alignment plan and building an optical system (excerpt from Guyer 2001).[1]

2. COORDINATE SYSTEMS

One of the first steps in planning the build of an optical system or related structure, such as an optical bench, is to define a coordinate system (sometimes called, e.g., the mechanical coordinate system or optomechanical coordinate system). This is also the case for optical component development. The coordinate system origin and orientation must be related to a directly measurable reference or referenced via transfer of measurable features. There are many ways of establishing a coordinate system, such as measuring optically-significant surfaces, hole features, and/or targets, or, in the case of components, parameters that define the prescription. Stable metrology features or fiducials that are mounted to the structure or instrument can then be calibrated and used as coordinate system references that are more convenient to measure during future alignment evolutions. Flat surfaces can be used to define planes parallel to that formed by two axes of the coordinate system. Points can be used to define an origin. If enough points are available (>=3) and well distributed across the space, a network of points can be used to reference the coordinate system in all six degrees of freedom (DoF). The features used to define the coordinate system should be measureable, environmentally stable, and accessible during the instrument build up and widely spread to reduce measurement uncertainties, especially if point targets are used to define angular DoF. After the coordinate system-defining features are measured (and metrology targets), the features are best-fit or otherwise transformed to nominal or ideal values used by mechanical and optical

designers. These values may come from configuration-managed (CM), computer-aided design (CAD) files, mechanical drawings, or, especially in the case of optical components, CM-controlled, optical ray trace files. The measurement of targets and/or features to "get into" the coordinate system is typically done at the beginning of the alignment process and is checked throughout various phases of integration and testing. Examples of coordinate systems for OSIRIS-REx Visible and IR Spectrometer (OVIRS) and James Webb Space Telescope (JWST) are discussed in this paper.

3. INSTRUMENTS

A large variety of measurement instruments and tools are available for optical alignment. Factors such as application (e.g., target access, line of sight), cost/availability, and measurement uncertainty requirements are used to help decide which instrument or system is selected. Risk to hardware health and safety is also critical in the selection.

Metrology systems can be classified into either contact or non-contact categories. For example, a laser radar (LR) instrument is a large volume tool for scanning mechanical or optical surfaces in a non-contact manner. A laser tracker (LT) instrument can also be used to scan or "tram" a surface to measure a plane or shape using the signal return from a spherically-mounted retroreflector (SMR) in contact with and dragged along the surface of interest[2]. Tramming is jargon for a contact technique for touching or dragging the SMR by hand across a surface while the LT measures points along the SMR's track of motion.

Metrology instruments can also be classified as systems that produce point-like data resulting in X, Y, Z coordinates and or systems that produce purely angular data, like vector direction cosines, with poor or no translational information. Some instruments can measure both angles and points, or some subset of six degrees of freedom. In the next few sub-sections, we discuss point-like (X, Y, Z) and angle measurement systems.

The instruments discussed here are not limited to the manufacturers whom we cite. Specific instruments and manufacturers mentioned or shown do not constitute an endorsement by NASA. Many manufacturers and models function in a similar manner and would produce similar results. We encourage the reader to study all available options.

3.1 XYZ Coordinate Measuring Instruments

This section describes contact and non-contact type instruments that primarily produce point like data that result in an X, Y, Z format. Angle measurements can be made or derived from the point data results of some of these instruments. The uncertainties of the angular data is typically much higher than instruments that are specifically designed for angular type measurements such as theodolites, etc.

The LT (Figure 2) utilizes an interferometric (IFM) relative distance and/or absolute distance meter (ADM) to produce range results, along with angular azimuth and elevation encoders to provide angular information in a spherical-type coordinate system[3,4]. The LT's red laser beam is ~mm across. The LT produces SMR position in spherical coordinates that is transformed into Cartesian coordinates by the software running the instrument. The SMR consists of a corner cube-type retro-reflector embedded in a precision "tooling ball" (TB). It is a high quality, steel sphere with low form error, accurately known radius, and specular finish. The center or apex of the corner cube is accurately located at the center of the TB. SMRs attach with high repeatability to metrology "nests" on the object being measured. Nests are three-point mounts that allow the SMR to seat in the nest in a highly repeatable manner. While nests come in a variety of geometries, they usually control the SMR center position with respect to a precision, mechanical interface (e.g., pin or bolt hole and plane around the hole). During data reduction, one uses knowledge of the SMR radius and any nest offset to find the point of interest on the hardware. As an aside, in our experience, it is extremely important to design the nest-to-hardware interface for maximum, feasible repeatability (e.g., precision pin hole for a tight, slip fit, ~<5μm clearance, somehow controlling clocking, and "spot-faced" mating surface). In addition, it is important to baseline targets that interface with the nest or nest-hardware interface that are interchangeable with targets for different metrology systems. For example, one might baseline the use of a LT and SMR/nest target concept, but, should an unexpected problem during later assembly make necessary

Figure 2. Laser tracker.

metrology using a coordinate measuring machine arm or photogrammetry system, if TB or off-the-shelf photogrammetry targets are available that have the same target-to-interface offset to high precision, one can realize savings in terms of schedule, budget, and stress. Flexibility of design requires perhaps extra effort during the design and planning phase and could incur slightly greater target cost, but can pay off later if problems arise.

Typical LT measurement uncertainties are approximately 10--25µm (1-sigma; accuracy) per meter of range along the horizontal and vertical directions (i.e., orthogonal to range), driven by uncertainty in the angular encoders, and about the same uncertainty in the range direction, but about constant in magnitude until factors like air turbulence and temperature uncertainty become important with increasing range. Uncertainties associated with the nest and the mechanical interface to the item under test further degrade accuracy. Advantages of LT systems are the large measurement volume capability and the ability to track a moving SMR into a target X, Y, Z location with live feedback of position. This tracking capability allows a network of three LTs to monitor the 6 DoF alignment of objects during dynamic operations, such as lifts or integration events, allowing one to track alignment and clearance in essentially real-time. The LTs are reliable, flexible instruments with a wide range of capabilities. With a network of tie points, LTs can be used in multiple stations (i.e., instrument positions) to decrease measurement uncertainties and measure of targets that would not be in the line of sight of the instrument from just one position. Disadvantages include a required straight line of sight from the tracker head to the target. SMRs are very expensive and may not be the best choice for a setup containing a large number of target nests. The SMRs must contact the target whether it be a nest or a surface that is being trammed. Safe access to targets may limit measurement capabilities. Usually, one needs two operators to perform LT metrology.

Figure 3 Laser radar.

The LR (Figure 3) uses LIDAR to measure range and uses azimuth and elevation encoders, similar to the LT, to measure the pointing direction of the beam[5]. The 1.55µm laser beam exits the LR with a diameter of about 40 mm, and is focused to a diffraction-limited spot down-range at the target of interest. The beam can be focused on and scanned across a surface. The LR is capable of scanning both matte and specular surfaces[6,7]. In addition, the LR measures the virtual center points of specular TBs by "peaking up" on the strength of the scattered and specular signal return. These tooling balls can be interchanged with LT SMRs --- i.e., they use the same nest mounts (Figure 4). The uncertainty in the range, horizontal, and vertical directions is approximately the same as the LT.

One advantage of using a LR rather than a LT is that it can help minimize human interaction with the item under test, because 1.) The LR uses tooling balls that are inexpensive compared to SMRs so the entire scene can be populated once and not disturbed throughout the measurements and 2.) the tooling balls do not require repointing when moving from station to station. In aerospace applications, the LR has also been used to measure some types of thermal blanketing for clearance envelope requirements. LR and LT instruments can be used together, in a network, with the LR measuring the spherical sides of SMR targets. Measurements with the LT and LR systems are made from multiple stations (positions) around the structure at varying heights. This helps to reduce any systematic uncertainties in the measurements. A LR system generally requires only one operator. One disadvantage is that, unlike the LT, the LR does not track moving targets. Both LT and LR systems can be used in metrology tests in support of environmental testing, such as thermal-vacuum exposure[8, 9].

Figure 4 SMR (Left) and TB (right) installed into metrology nests.

Another useful, but rare, large-volume measurement tool is the cathetometer. The cathetometer is a simple, non-contact instrument that consists of a telescope with an internal, crosshair reticule mounted to a precise, ~meter-sized, X-Y stage system. The telescope base ray is highly orthogonal to the X-Y plane of translation. One might think of the cathetometer as an alignment telescope with a very large translational range. One dimensional versions are more common. Cathetometer measurements yield results in only one or two DoF. Typical measurement uncertainties are on

the order of 100 μm or more, depending on the target type, illumination, etc. The uncertainty is also a function of factors such as cosine error, encoder resolution, target distance, and the user's alignment of the crosshair to the target. Some advantages of the cathetometer are the ease of use and ability to measure almost any type of target that can be seen through the telescope. Disadvantages of cathetometers are the fact that they are bulky and the measurement area is limited to the stage travel. Another disadvantage is that, in some applications, alignment to the target plane can be critical to prevent cosine error in the measurement, although this can be solved by using other metrology to measure the cathetometer measurement plane with respect to the target plane. A cathetometer can be combined with a high precision rotary stage to provide the cathetometer with different views of an article under test, providing six DoF alignment information.

Coordinate measuring machines (CMM) come in various forms. They use precision stages to move a probe in a three dimensional volume. Calibration turns encoder feedback into accurate information on the probe tip center's location within the volume. Further data reduction allows one to infer point or surface location for the item under test. There are contact and non-contact versions, depending on the probe design, and some have interchangeable heads for various probe options. One advantage of these systems is that the measurement uncertainties can be as low as the sub-micron level. A few disadvantages would be the limited volume and possible limited line of sight access to targets on multiple sides of the test item. In **Error! Reference source not found.**, we show a large CMM (Leitz[10]) with a contact probe that was used to measure features on the JWST primary mirror segments before installation to the backplane.

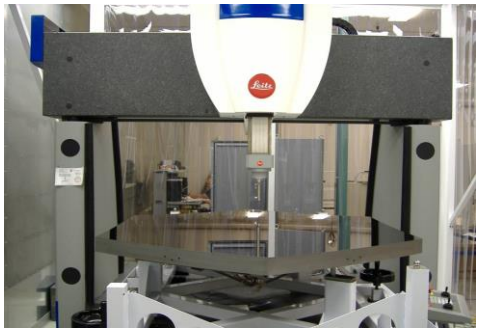

Figure 5 Leitz CMM measuring one of the JWST primary mirror segments (Tinsley, Richmond, CA).

Another, CMM-like tool available to the engineer are portable arms. These are available in various lengths and configurations. The arms are typically contact the item under test and utilizes multiple types of probe tips to make measurements. There are non-contact options for some arms such as laser scanner heads. One limitation is the measurement volume limited to the arm length from a fixed base (~meter). The measurement arms have the advantage that they can measure features that a LT or LR may not have a line of sight to from its stand. The measurement uncertainties are at best a few times worse than LT and LR systems and tend to degrade as a complex function of distance from the base.

For smaller systems and components, digital microscope-type metrology instruments offer an accurate, non-contact solution. They can be used to centroid on various types of features such as machined holes, metrology targets, edges and a multitude of other targets, including optical surfaces and large-format detectors. The advantage to these systems is that they are highly accurate (on the order of a few tens of microns at worst). Another advantage is that they can be used for electronically- and contact-sensitive parts such as detectors and MEMS devices. A few disadvantages are the limited measurement volume and the line of sight limitations of having to look down at the part on the platen surface.

Photogrammetry (PG) is a metrology technique with a long history. In "close range" PG, images of field of targets are obtained by a camera or network of cameras from a variety of different camera angles. Data reduction software identifies targets or other features in the images and solves for target position (and camera position) via a triangulation and adjustment algorithm. Cameras are sometimes hand-held or mounted and remotely controlled. Close range PG targets consist of a precision circle (or other formation) of small, retro-reflective spheres embedded in a substrate. Targets can be designed to be interchanged with metrology nests used for LT and LR measurements. The PG system takes multiple photos from various angles and orientations around the test article. Scale bars are placed around the hardware such that they have good visibility. Some targets are placed into the scene purely to assist the data reduction algorithm to identify images and generate a solution. After transformation to an X, Y, Z coordinate system, typical measurement uncertainties can be as low as 15--20μm (i.e., precision). PG is extremely tolerant of vibration and other instability, because the field of targets needs only be stable over the duration of a camera flash or other short exposure. A disadvantage to PG system is that it, like the LT, a target must be measured, as opposed to measuring the mechanical or optical surface directly.

Optical systems and modern aerospace structures tend to be made from materials that are impossible or extremely difficult to repair during integration (e.g., glass, composite). Regarding hardware safety and LT, LR, and PG systems in particular, we have found it important to find ways to secure the sometimes massive targets to their nest or the hardware under test using tape, small bolts, clamps, and/or tether-like designs. Some solutions for positive capture are available off-the-shelf. One should weight the risks --- care should be taken that the retention system not pose more of a risk to the hardware than a bare target.

The point source microscope (PSM)[11] (Figure 6) is another tool that has been found useful in aligning optical instruments. The PSM, first described in 1900 by Drysdale[12], produces a spherical wavefront for the system under test, while imaging the focal point of the return. A reflective sphere whose center is placed at the focal point of the objective will auto-reflect the beam back (Figure 7).

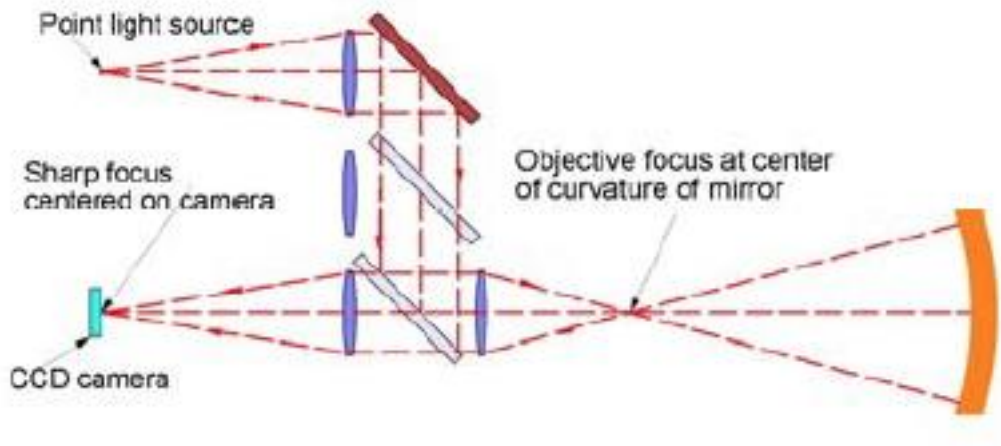

Figure 6 The objective focus of the PSM aligned with the center of curvature of a spherical mirror that is under test.

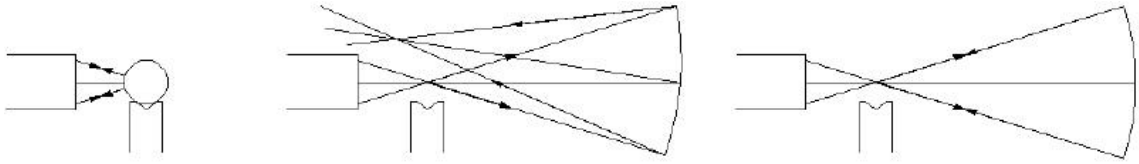

Figure 7 The use of a reflective sphere, which can be an SMR or TB, to align the focal points. The sphere can then be located in the master coordinate system using various metrology systems (diagram from Parks, 2015)[13].

The PSM allows quick location of the focus or center of curvature of an optic. Figure 7 shows a basic concept of locating the center of curvature of a spherical mirror. In this case the PSM location and orientation is adjusted until it is aligned (Figure 7, center and right diagrams). Software is used to monitor adjustments during alignment. Once aligned, a TB or the back surface of an SMR can be positioned as shown in the left image of Figure 7. Alignment of the TB or SMR is achieved when the center of the sphere is at the center of curvature of the spherical mirror or at the focus of the PSM objective which should be the same at this step. After alignment, a LT or LR can be used to measure the mirror fiducials with respect to the center of curvature. Similarly, this setup can be used to measure the focus of off-axis parabolic (OAP) mirrors and other optics. For the case of the OAP, this would be done by aligning the PSM so that the focus of the objective passes through the OAP focus. The diverging rays would hit the mirror and be collimated. A flat mirror would be placed in the beam path to return the light through the system.

The PSM is small and easy to setup and align to most optics. The objective can be changed to vary the numerical aperture of the output. The wavelength output is 632nm. Typical accuracies are not as good as an interferometer, but are on the order of a few microns. At GSFC, projects such as LCRD has successfully used this instrument to aid in alignment of flight instruments.

3.2 Angle Measuring Instruments

This section describes some instruments designed primarily for angular type measurements. Some of these instruments can be used to produce point-like data either by direct measurement or derived from angular data. The point measurement uncertainties in either case is typically higher than instruments that are designed to produce point-like data.

Autocollimating theodolites are typically used for optical cube and flat optical surface measurements. Theodolites send collimated light to its target that when aligned to the surface normal is returned collimated back through the telescope. Alignment is achieved by adjusting the azimuth and elevation of the theodolite until the returning image of the illuminated crosshair is aligned with the reticle crosshair in the eyepiece. Typical 1-sigma uncertainties are on the order of 10 arcseconds (i.e., accuracy; precision is typically 2 arcsec). Some LTs, such as the Lieca AT401 and AT402, will measure flat optical surfaces via reflection as well. The uncertainties are on the same order as that of the theodolites.

Theodolites can also be used to measure X, Y, Z, the three DoF translational location of targets like points on a structure using a triangulation technique. An array of theodolites is used to record the angular station of each target on the item under test, with two or more theodolite sightings per target. Large diversity in angle ("apex angle"), a large number of measurements, and different operators can provide uncertainties in position of about 50—100 μm or so for ~3 m-class measurement volumes. Scale bars are an important part of the setup and contribute to the uncertainty. In recent years, we have shied away from this cumbersome, labor-intensive, and time-consuming technique.

Total stations are similar to theodolites --- capable of measuring angle (including mirrors via autocollimation), but also point-like data using an internal ranging tool, like a distance measuring, visible light laser. Its typical uncertainty for angular measurements is similar to that of a theodolite, while the range measurement uncertainty is better than <1 mm (considerably better for some target types, but not as good as a LT or LR).

Figure 8. Autocollimator.

GSFC also maintains an inventory of "heritage" optical tooling instruments, similar to the cathetometer and theodolite in vintage, but with more specific application.

Autocollimators (AC) are autocollimating telescopes similar to a theodolite with base ray aligned accurately to the instruments barrel (Figure 8). An AC is primarily used to precisely measure angle (e.g., to calibrate other instruments, mechanisms). They have a resolution of 0.01 arcsec with a range of about ±1 arcmin.

Alignment telescopes (AT) are similar instruments that are often used to define or fix a line of sight for an optical system (Figure 9). ATs come in fixed, one-axis, and two-axis models. The later two have micrometer drums that allow for horizontal and vertical distance measurement perpendicular to the line-of-sight to a resolution of 0.0025 mm with a range of ±2.5 mm. Alignment telescopes are frequently paired with "pip" generators which allow for their use in aligning multiple optical elements within a system. The return image of the pip source provides feedback to the operator on the tip/tilt and centering error for both reflective and refractive optical systems. Alignment telescopes frequently have an autocollimation attachment, so, when set to infinity focus, the line-of-sight can be set normal to a reference mirror.

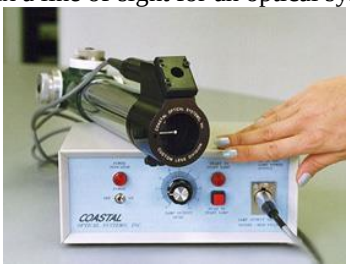

Figure 9. Alignment telescope with pip generator.

Other optical instruments are tilting levels and jig transits ((a) **(b)** **(c)**

Figure a and 10b). The tilting level is used to define a horizontal plane (i.e., a plane perpendicular to the gravity vector) with the capability of measuring deviations of targets from that plane within a range of ±2.5 mm to a resolution of 0.0025 mm via a parallel-plate micrometer. The jig transit is similar, except that it is used to define a vertical plane. It also has a "cross-telescope" that provides the capability to determining perpendicular line-of-sight to the plane.

(a) (b) (c)

Figure 10. (a) Tilt level, (b) jig transit, (c) optical plummet.

The optical plummet is shown in (a) **(b)**
(c)

Figure c. This device is essentially two small, autocollimating telescopes configured such that one points down and the other points up --- "anti-parallel" to each other. This provides the capability to align vertical systems that provide an autocollimation return. When paired with a mercury pool mirror (i.e., a gravity reference standard), the optical plummet can define a line-of-sight parallel to the gravity vector.

3.3 Instrument Applications

The following brief examples are taken from the JWST and OVIRS projects. Both projects will be described in more detail in Section 6. The examples below focus on how some of these instruments can be used.

The goal of metrology performed with the above instruments is to estimate the locations and orientations of the optical surfaces in an optical system. In some cases, instruments can sample the optical surfaces directly. In many cases, we rely on fiducials --- engineering features added to a component or subsystem that have a known relationship to the optical surface or conjugate of interest in some number of DoF. The arrangement, tolerances on, and types of fiducials are derived from a system tolerance analysis, the alignment plan, and the types of metrology tools available. We present a few example applications:

Figure 11. Detector measurement using Micro-Vu system.

An optical, non-contact CMM/microscope (Micro-Vu[14]) was used for JWST, OVIRS, and other projects to measure detector fiducials with respect to metrology targets on the assembly housing and the mechanical interface before integration to the instruments (Figure 11). In each case, the detector assembly incorporated measureable features that could be used at the subassembly level and after installation to the flight bench. The Micro-Vu system measured those features, along with the detector fiducials on the array. This information was used to calculate the shim dimensions to place the detector at the science instrument's predicted focal surface.

A cathetometer was used for the JWST ISIM (Integrated Science Instrument Module) project to measure optical pinhole features with respect to TB/SMR target nests[15] on the Master Alignment Test Fixture (MATF; Figure 12). The cathetometer was used, because it could measure small, pinholes that could not be easily measured using other systems, but could be seen through the cathetometer telescope eyepiece. A network of theodolites was used to align the cathetometer measurement plane to the MATF

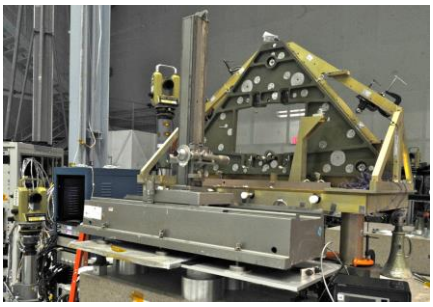

Figure 12. Cathetometer measurement of the JWST MATF.

Figure 13. PG camera.

target plane to minimize cosine error. As a check, the LR was used to scan some of the pinholes and the results agreed to within uncertainties.

We used a cryogenic PG system to measure the ISIM structure at cryogenic temperatures (~40 K)[16]. The system consisted of a boom within a large vacuum chamber with two PG cameras on opposite ends (Figure 13), protected by their own enclosures. The measurements were compared to LT/LR system results at ambient temperatures by interchanging the PG targets with metrology nests. The measurement helped check our model of how the structure changes as a function of temperature (i.e., optical metering structure characterization).

For the JWST project the LR was used to scan one of the primary mirror segments. There were two goals for the test. The first was to scan the edges of the mirror segments. This was needed to check mirror position once installed to the telescope backplane. This was done with some success. The scans results showed some uncertainty due to the edge of the mirror. The size of the incident laser beam on the edge limits the resolution. The second goal was to scan the mirrors front surface. This was done successfully. Despite the surface being specular. In fact, the LR was able to scan the mirror successfully from several vantage points around the mirror. The resulting scanned points were best fit to the shape of the primary mirror

Another interesting application of the LR involves mapping CCD pixels into a coordinate system. This work was conducted for the JWST during a research and development effort to measure the optical references on the science instruments. The goal was to place the CCD at the nominal entrance pupil of the instrument. To do this the CCD pixels were mapped to several metrology targets on the CCD housing. The process involved pointing and focusing the LRs laser onto a location of the CCD. A surface point measurement was made with the LR of that spot location. The CCD then took an image of the beams spot. The LR then measured the metrology targets on the housing. This relates the location on the CCD with the metrology targets in the same CS. This process was repeated by pointing the LRs laser to several more spots on the detector and repeating the previous steps. Using image analysis the spot centers were related to the XYZ measurements of the LR system and the metrology targets. This gave the ability to use the metrology targets to position the CCD plane onto the science instruments entrance pupil.

4. COMPONENT AND SUB-SYSTEM ALIGNMENT

This section provides a detailed discussion of an example of how a variety of these instruments were used for optical alignment and element characterization.

4.1 Component-level Metrology

Building and aligning an optical instrument generally consists of first defining a bench coordinate system, then element or subsystem characterization (i.e., lenses, mirrors, filters) followed by integrating and alignment of the components to the bench. Elements can consist solely of optical surfaces such as lenses, mirrors, etc. Elements can also consist of opto-mechanical subassemblies such as mechanisms and detector housings. This section discusses how system alignment is achieved by starting with component characterization and ending with system-level integration and alignment.

Element characterization for optical components such as mirrors and lenses for alignment can be done in two stages --- by manufacturing fiducials or features that can be measured easily using metrology tools at later stages of assembly and characterizing the relationship of those fiducials with respect to the prescription of the element. Examples of fiducials include flat surfaces that are diamond turned or polished to be reflective and machined holes. They could also be etch marks that define the location of some first-order property of an optical element such as the optical axis, aperture center, etc. Selecting the type of fiducial depends on factors such as manufacturability, available measurement tools, and uncertainty requirements. The required number of DoF and uncertainty for each must also be considered when planning the type and layout of fiducials. For example, if angular adjustment is important, then perhaps mirror-like, plano surfaces would work best, if an autocollimating instrument is available. If position is important, and a LT is available, then fiducials consisting of machined holes for target nests may be the best choice. If a part is rotationally symmetric, then perhaps the clocking or roll DoF need not be fiducialized. However, if one decides that a particular “optical DoF” (e.g., clocking/roll) is not important, one should consider whether neglecting a fiducial for that optical DoF might degrade the uncertainty in other, mechanical DoF via a cosine effect, because we build most systems in six DoF and

fiducials may not always be aligned with the optically-significant parameters of an element or system. The fiducials should allow access to the paraxial properties or optical surface(s) for the element. The difficult work is often the calibration of fiducial placement with respect to the optical surface(s) or paraxial properties of interest. We have encountered optical elements with fiducials, but no information on the connection between those fiducials to the properties of the element that we were required to align. Sometimes, the fabrication of the fiducials and optical surfaces is accomplished via the same means and even in the same setup --- this can lead to very low uncertainties and calibration may not be necessary, outside of a cross check. However, this is often not practicable and properties such as focus or pupil location and optical axis or chief/base ray pointing direction need to be separately measured and related to the element's fiducials' location and/or orientation "calibrated" --- i.e., values assigned based on the optical features of interest and with respect to a local coordinate system on the element. This might be accomplished via direct metrology of the optical surface(s) (e.g., via CMM) or a more sophisticated optical test using interferometry or an image-based test. Two types of fiducials are shown in Figure as an example. Both were used on OVIRS which will be discussed later. The figure on the left shows an assembly of three metrology nests with tooling balls installed for LR measurements. The center feature is a spherical, mirrored lens. The right image in Figure 14 shows a precision, machined hole located on the OVIRS, off-axis, parabolic primary mirror that can accommodate a metrology nest or can be measured directly using the LR hole point routine. Redundant fiducials of the same or different types can be beneficial in that it allows cross-checks of the measurement data using another system. It also provides a back-up if line-of-sight is lost to any particular fiducial during Integration and Testing (I&T).

Figure 14. Tooling balls inserted into metrology nests (left image) for the OVIRS surrogate field stop. The right image shows a precision machined hole used for a mirror fiducial on OVIRS.

Another method of characterizing optical elements is to directly measure the surface of the element via a non-contact method. A non-contact or low-force CMM or LR can be used to scan optical surfaces to measure the surface shape and location. Fitting the measured points can result in effectively determining paraxial parameters like the focus location, optical axis, and edge of the clear aperture, particularly when coupled with straightforward, geometrical optical modeling. The LR method is not as accurate as other techniques, like a high accuracy CMM, but has the benefit of not contacting the optical surface and can be done quickly and at a safe distance from the hardware.

For flat mirrors, several instruments and techniques are available to measure the location and orientation. If position is not important then a theodolite can be used. One approach feasible with several types of instruments is the "direct and through" technique[17]. This technique can be accomplished using a LR or LT to measure a SMR or tooling ball seen "directly" and "through" the mirror (i.e., its virtual image). The two measurement points and location of the instrument are used to calculate the position of the plane of the flat mirror and its surface normal orientation in the instrument's coordinate system. The angular measurement uncertainties are on the order of 10--15 arcsec, but is highly dependent on the test setup. The Leica LT401 laser tracker can measure the position and orientation of flat optical surfaces directly using its "mirror shot" mode. Its angular uncertainties are similar to, if not slightly better than, the direct-and-through technique. One major benefit to using the direct-and-through method or using a LT with reflective surface measurement capability is that the measurements can be easily related to a mechanical coordinate system. Using theodolites requires using other methods to transfer the measurements to a coordinate system. Relating the pointing direction of a flat mirror

fiducial to the optical parameters or surfaces of an element is often a custom arrangement, requiring an interferometric or image test setup and creativity on the part of the engineer.

Detectors can be characterized by implementing fiducials on the housing that are accessible after the detector is installed. The housing fiducials can be measured using a non-contact method of measurement with respect to the fiducials manufactured on the detectors active area, assuming that the manufacturer has placed fiducials on the detector surface and provided offsets to the active pixel array. If there are no fiducials provided by the detector manufacturer, then non-contact scans of the detector surface may be possible using a LR or LT or CMM arm with a scanner attachment, and these solutions may be very rough and subject to systematic error when attempting to measure such an unusual surface. In addition, alignment in-plane to the detector may be highly uncertain. If a non-contact metrology system is unavailable or does not meet the uncertainty requirements, there are AT- and image-based techniques that are feasible. Once characterized, the housing fiducials can be used to position the detector very easily in 6 DoF using a LT or LR system. . Regarding hardware safety --- when considering a metrology system that illuminates a detector, it is important to review the detector's irradiance requirement and consider possible mechanisms that could degrade the sensor's performance from measurement.

Mechanisms are a common subassembly for optical systems. Selectable pupil mechanisms that contain multiple filters or masks are common. Alignment of these mechanisms can be critical depending on the application. With proper forethought and fiducials mechanisms can be characterized and the position of key elements calibrated. The characterization results can be used to align the assembly into an optical system. IRMOS (Infrared Multi-Object Spectrometer) used a setup consisting of a cathetometer and theodolites to measure and align gratings in a wheel mechanism[18].

4.2 Sub-system level metrology

Once each element is characterized, they are integrated and aligned to the optical bench or system. A logical order of installation should be considered based on verification approach, accessibility, element availability, and other factors. Alignment can be divided into in phases of gradually higher precision until the required alignment error or performance is met ("align to a mm, align to a μm, align to a nm"). A large volume metrology system, like a LT or LR, can be used to measure each of the element's fiducials after the element is mounted, perhaps with pre-customized shims or interfaces based on earlier, as-built bench and element metrology. Adjustments can then be made to position the element at the nominal location based on the bench coordinate system and element characterization results. LT systems are excellent for this type of measurement and alignment iteration, since changes in point location can be viewed in real-time to give immediate feedback to adjustments being made. Other techniques involving interferometry, imaging, or wavefront sensing can be used in some applications to align to tighter tolerances when coupled with ray trace modeling.

A very useful method called "Trans-Track" can be used to measure the 6 DoF change in pose of hardware in real time[19]. The techniques requires three LTs that measure three SMRs simultaneously. This technique was used on the JWST project several times to monitor the movement of large hardware during installation.

5. ANALYTICAL TOOLS

There are a wide range of analysis tools available to process measurement data and generate statistics. GSFC uses commercial software packages such as Spatial Analyzer[20] (SA) to collect and process measurement data from various instruments such as the LT and LR systems. It should be mentioned that there are other software packages with similar capabilities to those of SA. The reader is encouraged to explore all options available. GSFC has also developed its own proprietary tool called OAFDAMS[21,22] to process theodolite and angular data using Microsoft Excel. Various custom routines have been developed at GSFC using tools like MATLAB® and Microsoft Excel to develop measurement statistics.

GSFC typically uses SA software to collect and conduct some processing of measured data from LT, LR and other systems. We internally coordinate and control the version of SA and other software that we use for instrument operation and data reduction. The software is able to combine the measurements and uncertainties from multiple instruments and thereby improve the overall accuracy of the resulting dataset. SA is also capable of handling measurement data from

other compatible instruments. GSFC uses SA to process scan data from the LR and LT systems. Scan data from the LR or LT can be fit to an assortment of shapes available in SA such as planes, spheres lines, etc. There are many examples of SA use on the JWST project. For example, the LR was used to scan thermal blanketing on one of the science instruments before installation to the ISIM structure to check for clearance in critical areas. The scanned measurement data from the LR was compared to an imported CAD model, which, by definition, used the same coordinate system, to check for critical clearances of the blanketing to other hardware.

GSFC uses several methods to improve and estimate measurement uncertainties and statistics. In most cases, measurements are taken from several stations and in multiple sets during testing. This data is processed in multiple ways depending on the application. In some applications, Spatial Analyzer is used to calculate measurement uncertainties using its USMN[23] algorithm. In other cases, the data is exported to excel and a Student's-t[24] uncertainty is calculated. In other cases, custom routines are written for specialized applications. For example, a custom Monte Carlo (MC) uncertainty propagation routine[25], written in MATLAB® for the JWST project was developed as a means to robustly propagate, analyze, and book-keep the uncertainty associated with spatially transforming targets and unit vectors between databases with common targets. The MC error propagation routine generates N-different geometric, best-fit transformations between two separate databases provided that there are at least three common targets in the two databases. Each of the geometric transformations involves simulating target measurements from the sum of the nominal targets and their randomly-drawn uncertainties. The randomly-drawn uncertainties are defined by the Student's-t probability density functions (PDF) for each of the targets in the databases. The 2-sigma standard deviation is calculated for all targets in the N-simulated MC transformations. The MC error propagation method has been shown to be beneficial for propagating uncertainty through multiple JWST databases and for estimating transformation uncertainty for line-of-sight modeling scenarios where one or more targets may be omitted from a best-fit transformation.

6. APPLICATIONS

In this section, we discuss two applications that cover both large- and small-scale optical systems. JWST is a large scale application where large-volume techniques are used to align the ISIM to Primary Mirror Backplane Support Structure (PMBSS) and Optical Telescope Element (OTE) structures. On the other end of the scale, the OVIRS instrument built for the OSIRIS-REx[26] (The Origins, Spectral Interpretation, Resource Identification, Security, Regolith Explorer) mission involves a much smaller scale alignment that utilizes the same alignment tools as JWST[27], as well as more traditional optical alignment tools. OVIRS involves the alignment of components such as mirrors to a small structure that is the optical bench.

6.1 JWST-Large Volume Metrology Application

The JWST project in general had call for many large-scale opto-mechanical and small-scale optical alignment applications. We discuss the large-scale alignment of the ISIM (containing the science instruments) to the PMBSS and OTE structure that supports the telescope mirrors.

Two major components of the JWST observatory (Figure) are the Optical Telescope Element (OTE) and the Integrated Science Instruments Module (ISIM). The OTE is the telescope that performs the light collection and initial image formation function. It includes the primary mirror segments, secondary mirror, aft optics, and the structural components that interface to each of the optics and to the Spacecraft.

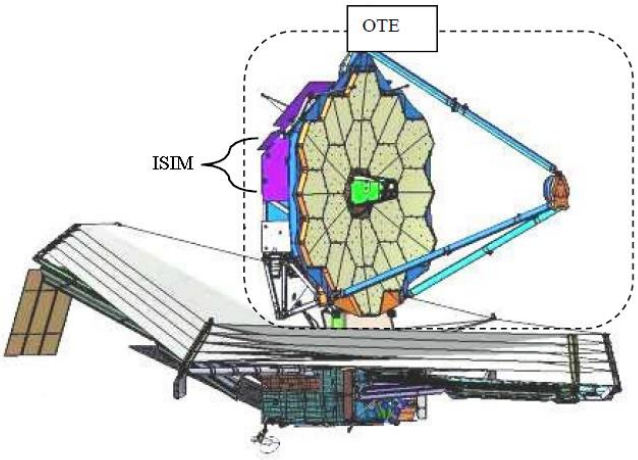

Figure 15. JWST Observatory showing the OTE and ISIM elements.

The ISIM is metered by a stiff, composite structure that houses a suite of science instruments (SIs) and other subsystem hardware. ISIM attaches to the Primary Mirror Backplane Support Structure (PMBSS) on the OTE with six manually adjustable kinematic mount (KM) struts that form a hexapod. During the testing phase of ISIM, prior to integration in to the OTE, ISIM was attached to a surrogate backplane structure called the Integrated Test Platform (ITP) with the six flight kinematic struts, shown in Figure with the SIs. Each of the kinematic struts attach to the respective kinematic seats on the ITP and PMBSS. Metrology nests are mounted to the base of the KM seats for knowledge of the seat locations for both the ITP and PMBSS.

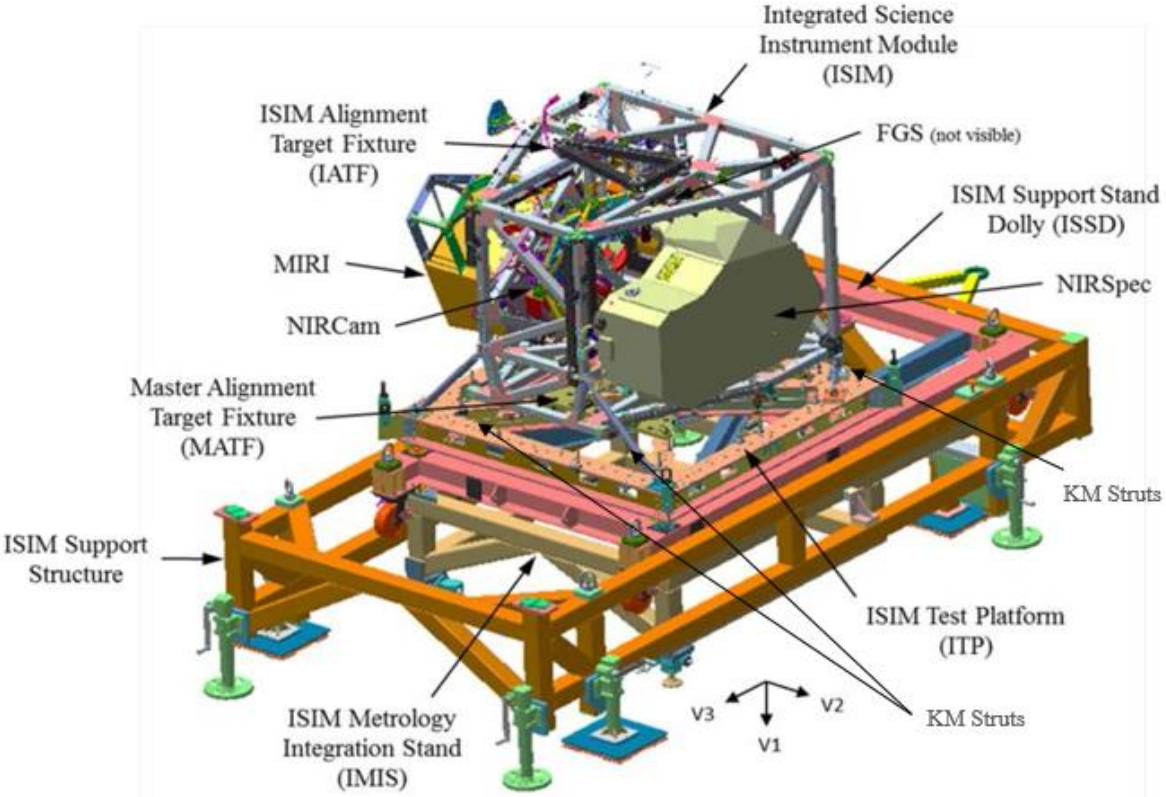

Figure 16. The Integrated Science Instrument Module (ISIM) attached to the Integrated Test Platform (ITP) with six kinematic struts (image from CAD). The SIs are shown installed to the ISM structure.

The goal of the OTE-to-ISIM integration was to install and align ISIM to the PMBSS structure to a nominal pose at ambient 1g to optimize the opto-mechanical performance of the observatory in an on-orbit, 0g, and cryogenic environment. In order to do this, the nominal ISIM pose at ambient 1g had to account for several different affects: 1) the ambient-to-cryogenic temperature shift between the alignment environment and on-orbit environment, which primarily affects KM strut contraction, 2) a coordinate system transfer from the ISIM structure to the OTE structure, and 3) the gravity change from 1g ambient alignment to 0g on-orbit.

The ISIM KM seat centers were calibrated separately using a CMM with respect to local mechanical references. Once the ISIM KM seats were integrated, the KM seats were calibrated using a laser tracker to measure mechanical surfaces with respect to external 38.1 mm TB/SMR nests (nests accept both laser radar and laser tracker targets) on the ISIM. With this calibration the ISIM KM seat locations can quickly be located by measuring the external ISIM targets.

Similarly the ITP KM seats were measured using a CMM and related to 38.1 mm TB/SMR targets around the seats. When the ISIM is measured on the ITP, the two sets of seat locations are known with respect to each other. The ISIM and ITP were measured using a combination of laser radars and laser trackers from multiple stations. ITP was utilized during environmental testing to determine potential shifts due to thermal, launch loads, etc. ITP could also have been used to verify ISIM pose changes due to strut length changes prior to the integration to PMBSS.

The PMBSS KM seats were measured using a calibrated tool which interfaced to the KM seat. The PMBSS KM tools are measured using laser radar to define the locations of the seats relative to the PMBSS coordinate system. In Figure , we show the PMBSS and ISIM structures during integration. The measurements with were made on the Ambient OTE Assembly Stand (AOAS) structure.

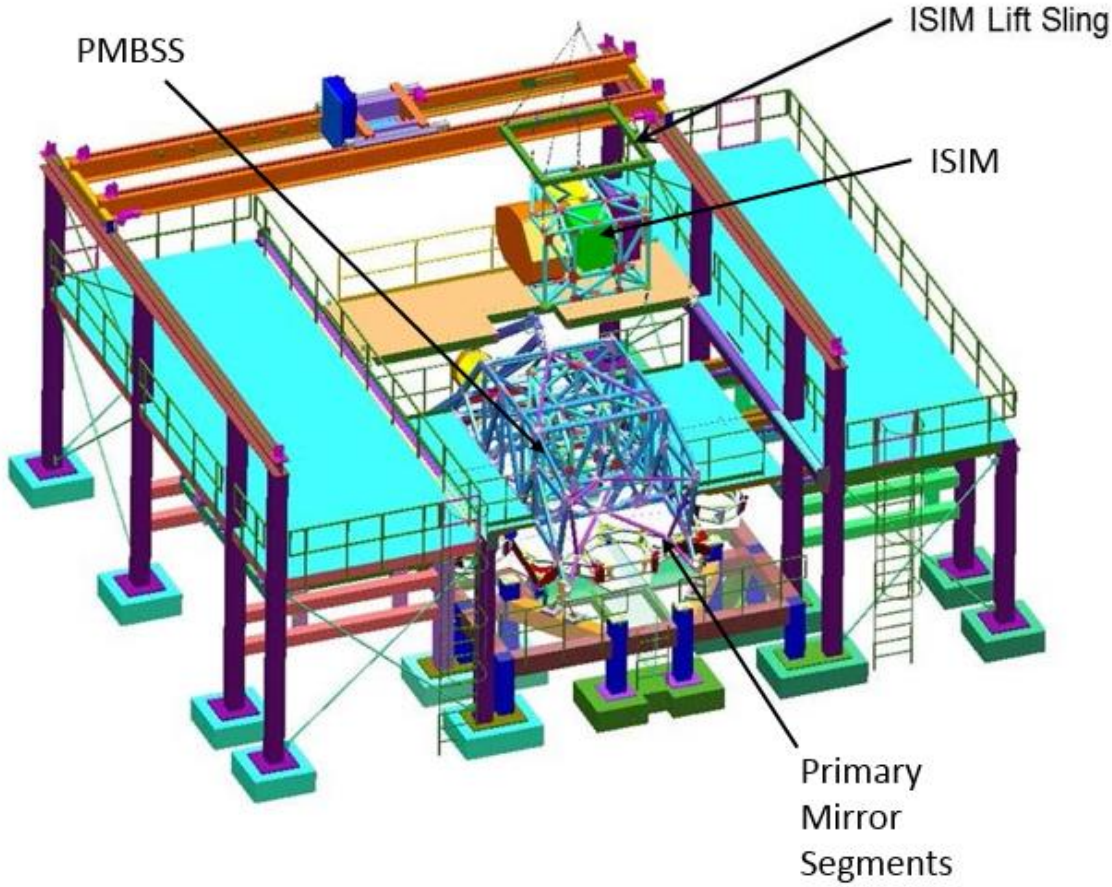

Figure 17. AOAS structure with PMBSS and the ISIM module (image from CAD).

For the analysis, two types of kinematic routines were developed in MATLAB® for kinematic modelling of the OTE-to-ISIM integration. The first routine was the Forward Kinematic Solution (FKS) which was used to predict the ISIM pose change as a function of strut length changes. The second routine, that we termed the Parallel Kinematic Solution (PKS), was used to predict ISIM pose change as a function of distortion changes in the six KM spherical strut seats on either the PMBSS stationary base or on the ISIM. MC routines, that iteratively called the FKS and PKS routines, were also developed to characterize ISIM pose change uncertainty as a function of uncertainty in the respective kinematic input variables.

6.1.1 Forward Kinematic Solution (FKS)

The FKS was used to predict the pose error of ISIM given known strut length adjustment errors in the 6 struts of ΔL. When the nonlinear function in Eq. 1. is minimized by iteratively searching for $\boldsymbol{C_{iter}}$ then a solution has been found for the pose change of the platform

$$f_{FKS} = \|(\boldsymbol{C_{iter}} * P_i) - B\| - L_i - \Delta L \tag{1}$$

where

- $\boldsymbol{C_{iter}}$ Composite 4x4 matrix representing rotations and translations about the X-, Y- and Z-axes that minimizes f_{FKS}.
- B Position of the 6 KM spherical strut centers on the stationary base.
- P_i Initial position of the 6 spherical strut centers on the adjustable platform.
- P_f Final position of the 6 spherical strut centers on the adjustable platform, where $P_f = \boldsymbol{C_{iter}} * P_i$
- L_i Initial measured lengths of the 6 KM struts.
- L_f Final nominal lengths of the 6 KM struts, where $L_f = \|(\boldsymbol{C_{iter}} * P_i) - B\|$
- ΔL Strut length error in each of the 6 KM struts, where $\Delta L = L_f - L_i$.

6.1.2 Parallel Kinematic Solution (PKS)

This PKS model was used to predict the ISIM pose error that would result when transferring ISIM from its surrogate base on the ITP to the prime base on the telescope PMBSS without changing the KM strut lengths.
When the nonlinear function in Eq. 2. is minimized by iteratively searching for $\boldsymbol{C_{iter}}$ then a solution has been found for the pose change of the platform as a function distortion in the spherical strut centers.

$$f_{PKS} = \|(\boldsymbol{C_{iter}} * P_i) - (B_i + \Delta B)\| - L \tag{2}$$

- $\boldsymbol{C_{iter}}$ Composite 4x4 matrix representing rotations and translations about the X-, Y- and Z-axes that minimizes f_{PKS}.
- B_i Initial position of the 6 KM spherical strut centers on the stationary base.
- B_f Final distorted positions of the 6 KM spherical strut centers on the stationary base.
- ΔB Distortion in in the spherical strut centers on the stationary base, where $\Delta B = \|B_f - B_i\|$
- P_i Initial position of the 6 spherical strut centers on the adjustable platform.
- P_f Final position of the 6 spherical strut centers on the adjustable platform, where $B_f = \boldsymbol{C_{iter}} * P_i$.
- L Fixed strut lengths, where $L = \|B_i - P_i\| = \|B_f - P_f\|$, for the 6 struts.

Note that an equation similar to Eq. 2. could be formed to model the platform pose change as a function of the distortion in the platform spherical KM strut centers (rather than distortion in the base spherical KM strut centers).

6.2 OVIRS-Small Volume Application

OVIRS[28,29] is a visible and near-infrared spectrometer instrument that will fly aboard the OSIRIS-REx mission when it launches in the Fall of 2016. The system consists of two OAP mirrors (primary and secondary), a field stop, filter array and a detector assembly (Figure 18). The optical path is highlighted in the figure. The three metrology nest locations shown are the base of the coordinate system. In general the integration and alignment was achieved in several stages. The first stage involved characterizing the components and optical bench. The second stage was the integration of each element to the optical bench using the results from the component level characterization. The third stage involved fine

tuning the system to achieve the optical requirements. At that point all of the alignment was completed at ambient temperatures. The final stage of alignment was conducted under cryogenic temperatures in a thermal vacuum chamber (TVAC). Since the flight detector is not operable at ambient temperatures the on-orbit boresight was not measured until TVAC testing.

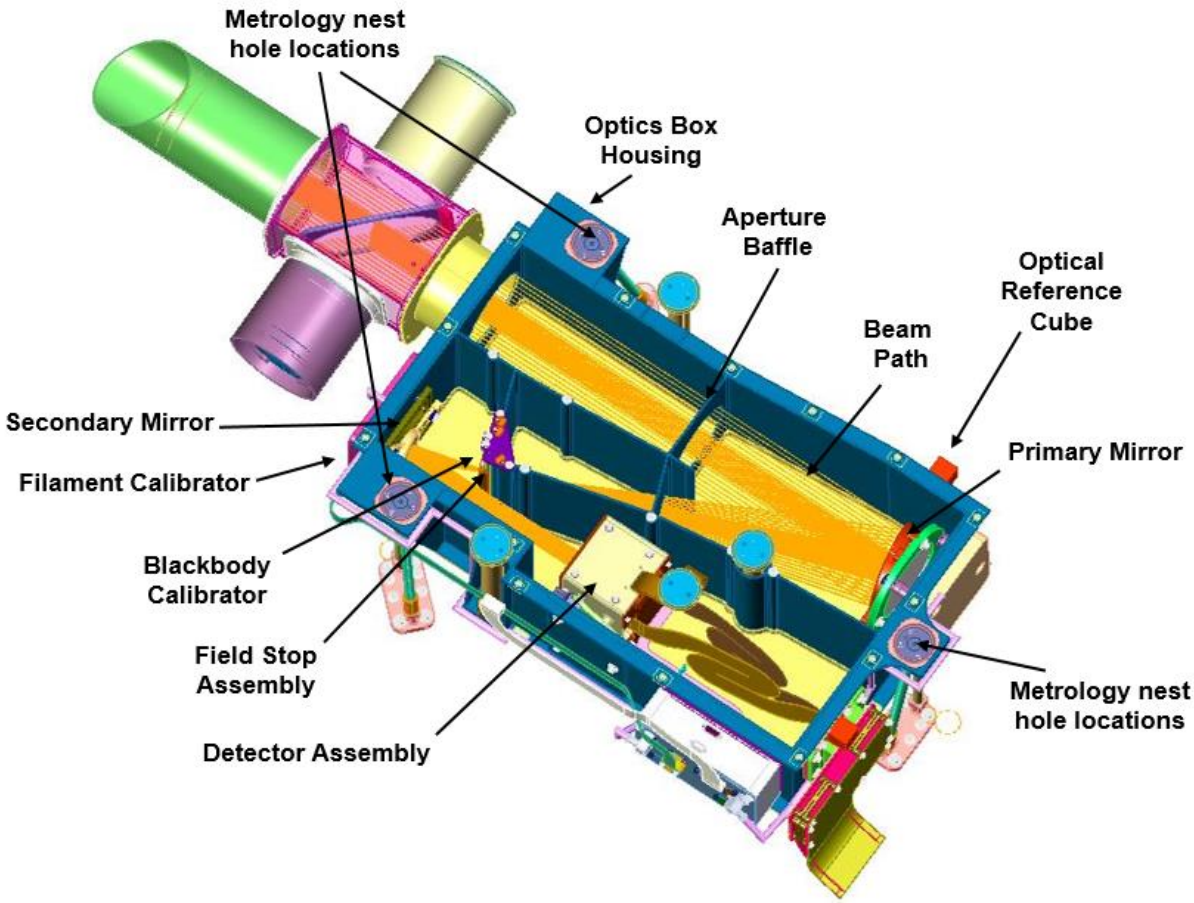

Figure 18. OVIRS optical layout showing the key features. The CAD image shows the beam path, optical reference cubes and metrology nest hole locations as well as the optical components.

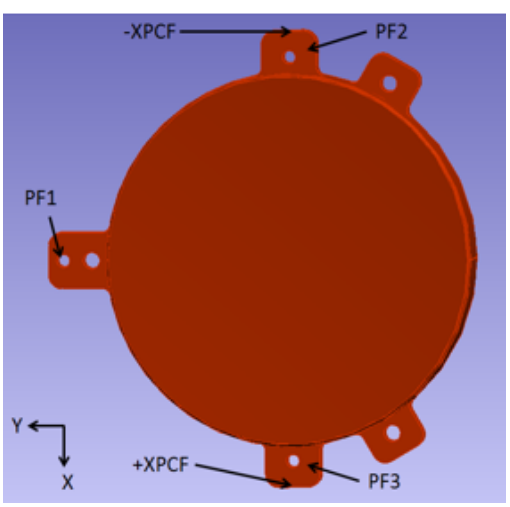

Figure 19. OVIRS primary mirror viewed from the front with fiducials shown.

Mirror characterization involved the manufacturer fabricating several fiducials on the primary and secondary OAP mirrors. Figure 19 shows the primary mirror with its named fiducials. The mirror consists of polished surfaces on the back of the mirror as well as edges of the PFx mounting hole feet. A coordinate system was defined for both mirrors to have its origin at the optical vertex of the parabola with the Z-axis pointed along the optical axis in the direction of the light propagation. The rear surface of the mirror was polished to a mirror finish and its normal defined the optical axis of the parabola. The three PF feet of the mirror were polished to define clocking about the optical axis. The PF1 foot surface normal (+Y) gives the direction to the parabola axis. Three precision holes (labeled PFx) were machined on the mirror feet to define position. The PF1 hole is located at a given distance along the Z-axis to the parabolic vertex. The manufacturer provided the coordinates of all of

the fiducials with respect to the first order properties of the mirror. The secondary mirror was built and characterized by the same process as the primary. The extra effort put into fabricating the fiducials paid off during component and system level alignment and testing. During interferometry measurements alignment of both mirrors to the interferometer was quickly and easily accomplished using several theodolites and a LT/LR system.

The field stop was characterized by using a laser radar to accurately scan the 1.4 mm diameter aperture with respect to three fabricated holes containing metrology nests with 12.7 mm diameter tooling balls. The three tolling balls were fabricated such that they would be visible to the LR or LT during installation to the optical bench. A surrogate field (Figure 20) stop was fabricated to assist in the alignment of the primary mirror. The surrogate field stop assembly was fabricated to be exactly the same as the flight unit except the aperture was replaced by a spherical lens coated with aluminum to provide a mirror-like finish. The center of the sphere was placed as close to the flight field stop opening location as possible. The surrogate sphere center to the flight field stop aperture location was measured by using the LR. This was done by mounting the flight field stop assembly to a stable repeatable mount and measuring the field stop opening. The flight field stop was replaced by the surrogate and the LR was used in its "Tooling Ball" mode to measure the center of the sphere. The difference of the field stop opening and sphere locations were used to calculate the proper shim values needed for proper alignment to the optical bench.

The detector assembly which includes the filters was fabricated to have several reference holes on the top of the assembly that would be visible while installed to the optical bench. As the detector was built up to the assembly level the detector was measured using various measurement tools and its location transferred to the detector assembly targets. At the final stage the Micro-Vu system was used to measure the filter aperture in front of the detector with respect to three machined holes (for metrology nests) that are located on the top of the detector housing for visibility when installed to the optical bench.

The integration and alignment of the components occurred in two phases. The first phase was the installation and alignment of the two OAPs and field stop. The detector assembly was installed in the second phase. This was merely due to the fact that the interferometer could not be used with the detector in place.

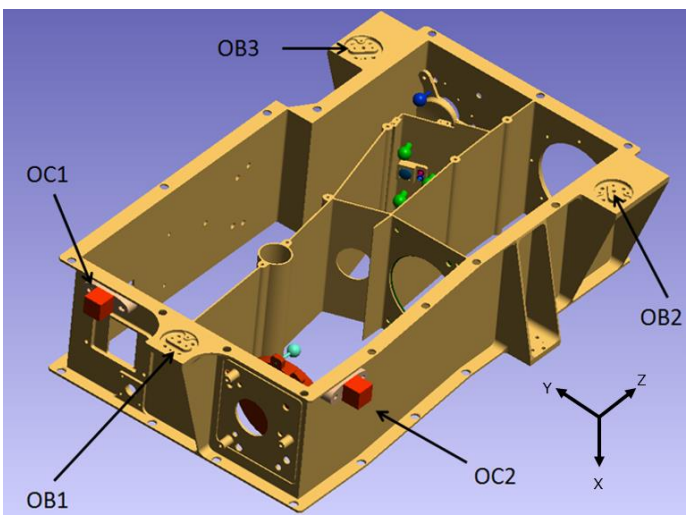

Figure 20. OVIRS optical bench with both mirrors and field stop installed. OBx targets define the coordinate system. OC1 is the primary cube.

Before the components could be installed the optical bench was characterized and its coordinate system defined. The optical bench contained two optical cubes and three threaded holes to house optical nests. Characterization involved measuring the three nest locations, all cube surfaces and the optical opening of the box with several theodolites and a LR system. The threaded holes used as the basis of the coordinate system is shown in Figure . These holes were accessible during all phases of metrology. The nests could be easily installed and removed when needed. The nominal coordinate system axes orientation is also shown in the figure.

Integration started with installing the surrogate field stop into the bench. The surrogate field stop was shimmed to place the center of the sphere at the flight field stop location on the optical bench. The surrogate field stop mirrored lens serves as a mean to return the beam in a double pass mode to the interferometer. The optical box and interferometer were leveled to gravity and roughly aligned to the interferometer output using the three metrology nests and optical cube. The primary mirror was installed to the bench and shimmed using the results of the component level characterization which defined the focus and the optical and parabolic axes with respect to the fiducials and mounting surface. The goal was to align the mirror to the already installed surrogate field stop assembly nominally. The optical bench was then aligned to the interferometer output using theodolites and the primary mirrors

rear surface. The initial alignment using this technique resulted in fringes being seen by the interferometer but was not optimized. Optimization was achieved in iteration by shimming and testing until the requirements were met at this stage.

Once the primary mirror was aligned the surrogate field stop was removed and replaced with the flight field stop. The secondary mirror was installed to the bench in the same manner nominally. In Figure , we show the test setup. A large flat mirror was used to return the beam through the system in double pass mode. Theodolites were used to align the secondary mirror and large flat mirror. After the interferometer measurements were complete the interferometer output beam was measured with respect to the optical reference cubes on the optical bench with theodolites to define the ambient boresight of the system.

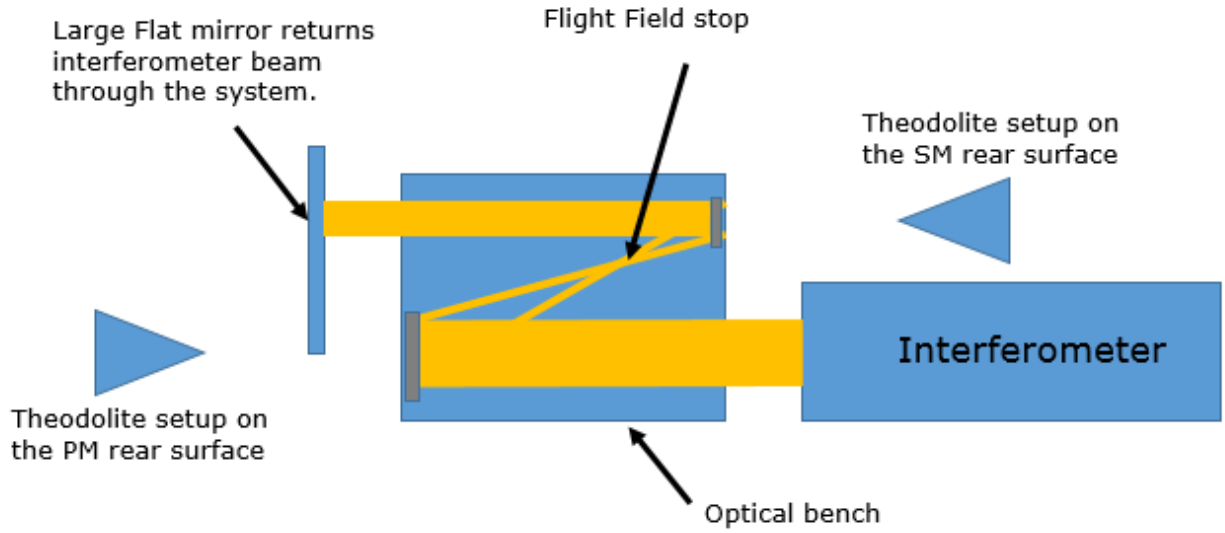

Figure 21. Interferometer setup through entire system with the primary and secondary mirrors installed (notional cartoon).

The final integration step from an optics perspective was to integrate and align the detector housing. The metrology nests on the detector housing were used for positioning within the box using the results of the detector characterization. A centering check was done by viewing the interferometric return of the filter face through the system.

The final step of measuring the optical boresight was accomplished during the full instrument level TVAC testing. Details of this test are beyond the scope of this paper. In short, at cryogenic on-orbit temperature the collimated source scanned the OVIRS field of view to determine the on-orbit boresight. At ambient temperature the boresight of the collimated source was related to the OVIRS primary cube in the thermal vacuum chamber via metrology using a Leica 401 series LT. The cryogenic to ambient shift of the structure and OVIRS instrument was factored in to link the ambient and cryogenic measurements.

7. SUMMARY

We discussed some basic tools for measuring and aligning an optical system or instrument. We listed several, newer metrology instruments to provide the reader with a summary of our experience and perhaps provide input as to their current and future applications. We hold that large-volume metrology tools such as LR and LT can also be useful for small-scale optical alignment and we provided examples of applications from several space flight projects, large and small.

Metrology tools, references, techniques, and data reduction algorithms must be considered early during the planning phase of the development of an optical instrument or telescope or precision assembly, like a spacecraft, and made an integral part of the alignment and integration plans. It is important to plan for change --- metrology-related aspects of

the plan should accommodate changes to the measurement scheme or the program's needs and be able to adapt readily to problems that inevitably develop during a one-of build.

The success of a metrology and alignment plan is reliant on attention to detail during all phases of a program's development. Details make or break an effort --- examples include designing for target interchangeability, designing targets or references on an element that capture all six DoF, adequately calibrating targets with respect to what we really care about (e.g., the optical surface, first-order properties of a system, important conjugates like focus or pupil, chief-ray related parameters, detector pixels), planning conservative line of sight during the design phase, adequately calibrating scale bars or other important references at the temperature needed, protecting target or reference access and line of sight during a build, updating error budgets as a build progresses, cross-checking measurements and data analysis, etc. The point about cross-checks cannot be over-emphasized: Humans and their tools are inherently fallible. Quality assurance measures associated with large institutions can only go so far in checking that we follow the processes that we establish --- they usually shed little light on whether those processes are correct or the best to address requirements. Furthermore, they usually cannot find subtle systematic errors in measurements or mistakes in calculations or analysis post-measurement. It is the responsibility of the metrology and alignment personnel to not only work with quality assurance to help make them effective at their role, but also build intelligent cross-checks into the work plan such that one has confidence in uncertainty estimates, there is low risk of hidden systematic error, and problems with alignment or uncertainty are detected before the build is complete, launch, or other significant gate.

Optical alignment is a broad subject, but we hope that this paper has added to the reader's toolbox a few ideas and techniques (or provided a seed for their own ideas) to not just align a system *precisely*, but also *accurately* --- i.e., to an absolute six DoF station within a coordinate system.

8. ACKNOWLEDGMENTS

This work is supported by NASA Goddard Space Flight Center and the James Webb Space Telescope project. Special thanks is given to the OVIRS, JWST, and LCRD teams and members of the NASA GSFC Optics Branch and Alignment, Integration & Test Group for providing technical input.

REFERENCES

[1] R. C. Guyer, A. Sanders. Lockheed Martin Co. "Optical Alignment Mechanisms," SPIE Short Course, 2001.
[2] R. Ohl, B. Hoffmann Eegholm, M. Casas, B. Frey, M. Dominguez, J. Gill, P. Morken, K. Redman, V. Roberts, B. Saif, and T. Scirpo, Metrology Trades for Ambient Testing of James Webb Space Telescope, Coordinate Metrology Systems Conference, 2009.
[3] Burge, J. et al., "Use of a commercial laser tracker for optical alignment," Proc. SPIE 6676, 2007.
[4] Gallagher, B., "Optical Shop Applications for Laser Tracker Metrology Systems," thesis, University of Arizona, 2003.
[5] Nikon Metrology NV, Leuven, Belgium.
[6] R. Ohl, B. Eegholm, and T. Slotwinski, Laser radar metrology for fabrication, alignment, and verification of large mirrors, SPIE Optifab 2011.
[7] B. Eegholm, W. Eichhorn, R. von Handorf, J. Hayden, R. Ohl, and G. Wenzel, LIDAR metrology for prescription characterization and alignment of large mirrors, Proc. SPIE 8131, 81310I , 2011.
[8] D. Kubalak, T. Hadjimichael, R. Ohl, A. Slotwinski, R. Telfer, and J. Hayden, Absolute Position of Targets Measured Through a Chamber Window Using Lidar Metrology Systems, NASA Tech Briefs, 2011.
[9] J. Hayden, B. Eegholm, T. Hadjimichael, D. Kubalak, R. Ohl, R. Telfer, and P. Coulter, Laser Radar Through the Window (LRTW) Coordinate Correction Method, provisional patent application number 61674985, 2012.
[10] http://www.leitz-metrology.com
[11] Optical Perspectives Group, LLC, 520-529-2950, www.optiper.com
[12] Drysdale, CV, Transactions of the Optical Society, Vol2, 1900.
[13] Parks, Robert E. "Autostigmatic microscope and how it works." Applied optics 54.6 (2015): 1436-1438.
[14] https://www.microvu.com

[15] Hadjimichael, Theodore J., et al. "Large volume, optical and opto-mechanical metrology techniques for ISIM on JWST." 2015 IEEE Aerospace Conference. IEEE, 2015.
[16] M. Nowak, P. Cleveland, A. Crane, P. Davila, A. Herrera, J. Hylan, A. Liehr, J. Marsh, R. Ohl, K. Redman, H. Sampler, J. Stock, G. Wenzel, R. Woodruff, and P. Young, Verification of the James Webb Space Telescope Integrated Science Instrument Module cryogenic structural alignment requirements via photogrammetry, Proc. SPIE 7068, 70680Q, 2008.
[17] S. Sandwith & R. Predmore, "Real-time 5-micron Uncertainty with Laser Tracking Interferometer Systems using Weighted Trilateration," New River Kinematics, Inc. Williamsburg, Va.
[18] S. Gutkowski, R. Ohl, J. Hylan, J. Hagopian, S. Kraft, J. Mentzell, J. Connelly, J. Schepis, L. Sparr, M. Greenhouse, and J. MacKenty, Alignment of the grating wheel mechanism for a ground-based, cryogenic, near-infrared astronomy instrument, Proc. SPIE 5172, 36, 2003.
[19] Hubler, D., et al. "Using Real-Time, 6D Object Tracking to Assemble Large Aerospace Components." 2000 CMSC Conference Detroit, Michigan. 2000.
[20] New River Kinematics, Inc., Williamsburg, Va.
[21] C. Aviado, J. Gill, K. Redman, and R. Ohl, Methods for correlating autocollimation of theodolites and coordinate metrology in spacecraft systems, Proc. SPIE 6273, 62733H, 2006.
[22] W. Eichhorn, "Optical alignment measurements at Goddard Space Flight Center," Applied Optics 21, 3891, 1982.
[23] S. Sandwith & R. Predmore, "Real-time 5-micron Uncertainty with Laser Tracking Interferometer Systems using Weighted Trilateration," New River Kinematics, Inc. Williamsburg, Va.
[24] J. Hayden et al., "Measurements and Analysis used for the Determination of the James Webb Space Telescope Integrated Science Instrument Module Vehicle Coordinate System," Coordinate Metrology Society Conference, July 2010.
[25] J. Hayden, M. Khreishi, T. Hadjimichael, and R. Ohl, Monte Carlo Method for Uncertainty Propagation in JWST Metrology Databases, Coordinate Metrology Systems Conference, 2014.
[26] https://www.nasa.gov/mission_pages/osiris-rex/index.html
[27]http://www.jwst.nasa.gov
[28] D. C. Reuter and A. A. Simon-Miller, The OVIRS Visible IR Spectrometer on the OSIRIS-REx Mission., 'NASA/GSFC, Code 693, Greenbelt, MD 20771, 2 NASA/GSFC, Code 690, Greenbelt, MD 20771.
[29] Simon-Miller, A. A.; Reuter, D. C. "OSIRIS-REx OVIRS: A Scalable Visible to Near-IR Spectrometer for Planetary Study," 44th Lunar and Planetary Science Conference, held March 18-22, 2013 in The Woodlands, Texas. LPI Contribution No. 1719, p.1100.